TISSUE ENGINEERING: Part A
Volume 22, Numbers 17 and 18, 2016

DOI: 10.1089/ten.tea.2016.0132

termis
Tissue Engineering
& Regenerative Medicine
International Society

ORIGINAL ARTICLE

Engineered Tissue–Stent Biocomposites as Tracheal Replacements

Liping Zhao, MS,[2,*] Sumati Sundaram, PhD,[1,2,*] Andrew V. Le, PhD,[2] Angela H. Huang, PhD,[1] Jiasheng Zhang, MD,[3] Go Hatachi, MD, PhD,[2] Arkadi Beloiartsev, MD,[2] Michael G. Caty, MD,[4] Tai Yi, MD,[5] Katherine Leiby, BS,[1] Ashley Gard, MS,[1] Mehmet H. Kural, PhD,[2] Liqiong Gui, PhD,[2] Kevin A. Rocco, MS,[2] Amogh Sivarapatna, PhD,[1] Elizabeth Calle, PhD,[1] Allison Greaney, BS,[1] Luca Urbani, PhD,[6] Panagiotis Maghsoudlou, PhD,[6] Alan Burns, PhD,[6,7] Paolo DeCoppi, MD, PhD,[6] and Laura E. Niklason, MD, PhD[1,2]

Here we report the creation of a novel tracheal construct in the form of an engineered, acellular tissue–stent biocomposite trachea (TSBT). Allogeneic or xenogeneic smooth muscle cells are cultured on polyglycolic acid polymer–metal stent scaffold leading to the formation of a tissue comprising cells, their deposited collagenous matrix, and the stent material. Thorough decellularization then produces a final acellular tubular construct. Engineered TSBTs were tested as end-to-end tracheal replacements in 11 rats and 3 nonhuman primates. Over a period of 8 weeks, no instances of airway perforation, infection, stent migration, or erosion were observed. Histological analyses reveal that the patent implants remodel adaptively with native host cells, including formation of connective tissue in the tracheal wall and formation of a confluent, columnar epithelium in the graft lumen, although some instances of airway stenosis were observed. Overall, TSBTs resisted collapse and compression that often limit the function of other decellularized tracheal replacements, and additionally do not require any cells from the intended recipient. Such engineered TSBTs represent a model for future efforts in tracheal regeneration.

Introduction

In adult patients, tracheal defects less than ~5 cm can generally be resected with primary reanastomosis of the native trachea. For longer defects, however, some sort of tracheal replacement is often needed.[1–3] Numerous approaches have been studied previously, including wholly synthetic materials,[1,3–5] allografts,[4–7] autografts,[1,6,7] and tissue-engineered decellularized tracheas.[1,4,8–10] All these options have been constrained by problems including tracheal collapse requiring repeated stenting, infection, and erosion into adjacent structures. Superior solutions are clearly needed.

Native trachea is a multilayered structure composed of C-shaped cartilaginous rings, a ciliated respiratory epithelium on the lumen, and connective tissue, including fibroblasts, smooth muscle cells (SMCs), and associated blood supply in the tracheal wall. Although the cartilaginous rings support the cylindrical shape and resist airway compression, the connective tissues enable the trachea to bend, expand, and bear tensile loads.[4–7,11,12] The epithelium comprises several different cell types such as ciliated cells, goblet cells, secretory cells, and resident basal cells that are integral to the epithelial repair and renewal process.[8–10,13,14] Characteristics of an ideal tracheal replacement have been said to include lateral rigidity, longitudinal flexibility, lining of respiratory epithelium, air-tight anastomoses, ability to integrate into adjacent tissue, no requirement for immunosuppressive therapy, and implantability using straightforward surgical techniques.[1,11,12,15] To date, no tracheal replacement has met all of these criteria.

Reports of utilizing allogeneic aorta for tracheal replacement have noted a universal requirement for stenting, and a significant rate of foreshortening of the grafts after implantation.[2,13,14,16] Clinical utilization of allogeneic tracheal transplantation has also been reported,[1,15,17] although this approach requires immunosuppression and surgical flap placement for tissue perfusion, and can lead to airway collapse and a requirement for stenting as well.[2,4,5,16] Clinical application of tissue-engineered, decellularized tracheas was first reported in

Departments of [1]Biomedical Engineering, [2]Anesthesiology, and [3]Internal Medicine Cardiology, Yale University, New Haven, Connecticut.
[4]Section of Pediatric Surgery, Yale University, New Haven, Connecticut.
[5]Nationwide Children's Hospital Research Institute, Columbus, Ohio.
[6]UCL Institute of Child Health and Great Ormond Street Hospital, UCL, London, United Kingdom.
[7]Department of Clinical Genetics, Erasmus Medical Center, Rotterdam, The Netherlands.
*These two authors contributed equally to this work.

2008.[9,17] Since the first report, more than a dozen patients worldwide have received decellularized airway replacements, and although these patients have not required immunosuppression, their outcomes have been complicated by repeated stenting procedures to maintain airway patency.[4,5,18,19] In some patients, investigators have attempted to speed cellular repopulation by systemic administration of granulocyte-colony stimulating factor, erythropoietin, and transforming growth factor beta.[3,9,20] In alternative efforts to provide an airway with sufficient rigidity while avoiding the need for a donor trachea, investigators have also utilized synthetic materials, such as a nanocomposite made from polyhedral oligomeric silsesquioxane that is covalently bound to poly-(carbonate-urea) urethane (POSS-PCU).[18–20] Patients have undergone tracheal grafting with cell-seeded POSS-PCU constructs with some success, although granulation tissue formation and esophageal erosion have been reported. Hence, although some notable clinical successes have been observed, existing technologies for tracheal engineering have been limited by problems with airway patency, tracheal collapse requiring stenting, infection, and erosion.

To overcome some of the limitations and problems with current approaches, this report describes a completely novel, engineered, acellular tissue–stent biocomposite trachea (TSBT) that can function well as a tracheal replacement. When implanted into rodents and nonhuman primates, the TSBTs are remodeled adaptively by the host, leading to the formation of a confluent epithelial layer and abundant microvasculature in the wall. Over periods of up to 8 weeks in 14 animals, no instances of airway perforation, infection, stent migration, or erosion were observed. Because they are stented, TSBTs resist the collapse and compression that often limit other decellularized tracheal replacements. Notably, TSBTs do not require any cells or tissue to be harvested from the intended recipient, and therefore may be developed as a readily available, off-the-shelf tracheal replacement.

Materials and Methods

Cell culture

Rat, bovine, or human aortic SMCs were extracted from aortic segments as previously described.[21] Cells were cultured in a Dulbecco's modified Eagle medium (DMEM)/10% fetal bovine serum (FBS) medium in a sterile environment at 37°C and 5% CO_2. Culture medium was replaced every other day, and cells were passaged approximately once a week. All cell culture reagents were purchased from Life Technologies (NY) unless otherwise stated.

Creating tissue–stent composites

A novel scaffold was first prepared by wrapping polyglycolic acid (PGA) mesh (Biomedical Structures, RI) around nitinol stents (Boston Scientific, MA) either as a single layer or as a double layer (stent sandwiched between two layers of PGA mesh). Scaffolds of various sizes were tailored to meet requirements for either small or large animal implantation studies. The polymer–stent composites were statically suspended on silicone tubing and cultured inside a bioreactor similar to procedures previously reported[22–24] for 8 weeks. Two million, passage 2, rat bovine, or human SMCs were seeded onto the scaffold constructs. The bioreactor medium was composed of DMEM (high glucose), basic fibroblast growth factor (5 ng/mL), epidermal growth factor (0.5 ng/mL), lactic acid (0.5 g/L), insulin (0.13 U/mL), penicillin G 100 U/mL, proline/glycine/alanine, $CuSO_4$ (3 ng/mL), and vitamin C (50 ng/mL), as previously described.[24] Total volume of medium in the reactor was $\sim$400 mL. Half of the bioreactor medium was changed two times per week and vitamin C was supplemented to the culture three times per week. Lactic acid was freshly added to the medium once a week (1 g/L). The engineered tracheal constructs were cultured in 20% FBS for the first 4 weeks, after which the serum was reduced to 10% of total medium volume.

Decellularization process

The engineered tissue–stent composite was decellularized by a multistep process.[24,25] First the construct was placed in a salt wash solution (1 M NaCl, 0.1 M NaOH, 25 mM EDTA) followed by treatment with a 2 U/mL Benzonase solution and a final treatment with 0.5% CHAPS solution. Constructs were placed in each solution for up to 6 h, with multiple washes with Dulbecco's phosphate-buffered saline between each step. After completion of the decellularization process, the TSBTs are stored in sterile PBS solution at 4°C until further use. All reagents were obtained from Sigma Aldrich, Inc. (MO).

Quantification of collagen content and sulfated glycosaminoglycans

Collagen was quantified with a colorimetric assay to detect OH-proline.[26] Samples were lyophilized and weighed, then incubated in papain at 60°C overnight (Sigma). Papain-digested samples were incubated in 6 N HCl at 115°C for 18 h, neutralized, oxidized with chloramine-T, and reacted with *p*-dimethylaminobenzaldehyde. Absorbance was measured at a wavelength of 550 nm and a 1:10 w/w ratio of hydroxyproline to collagen was used to calculate the collagen content of the tissue. At least three samples were analyzed for native and decellularized samples.

Sulfated glycosaminoglycans (sGAGs) were quantified using the Blyscan GAG assay kit (Biocolor). Papain-digested samples (prepared as already described) were assayed according to manufacturer's instructions. Note that the TSBT scaffold utilized in this analysis did not include the stent material.

Mechanical characterization

Biomechanical tests were performed on native and engineered tracheas. Tensile and compression tests were performed using an Instron 5848 (Instron, Inc., MA) equipped with a 100 N load cell to obtain stress–strain relationships. Stress (σ) and strain (ε) were obtained from the cross-head force (F) and displacement (ΔL) measured by the test machine as $\sigma = F/A$ and $\varepsilon = \Delta L/L_0$, where A is the area over which the force is applied and L_0 is the original length of the sample. Young's modulus (E) for the tissue was determined by the slope at the linear regions of the stress–strain curves.

Immediately before the mechanical tests, the characteristic morphometric dimensions of each sample were measured: thickness (t), height in the direction perpendicular to the applied load (h), and length in the load direction (L_0c for the compression tests and L_0t for the tensile tests).

Average and standard deviation (SD) values of these three morphometric parameters for tension are $t = 0.46 \pm 0.17$ mm, $h = 1.89 \pm 0.44$ mm, $L_0t = 5.07 \pm 0.66$ mm for native rat trachea; $t = 0.33 \pm 0.05$ mm mm, $h = 2.68 \pm 0.46$ mm, $L_0t = 2.64 \pm 0.71$ mm for decellularized rat trachea; $t = 0.41 \pm 0.05$ mm mm, $h = 4.93 \pm 0.61$ mm, $L_0t = 3.64 \pm 0.47$ mm for engineered rat trachea. Average and SD values of these three morphometric parameters for compression are $t = 0.48 \pm 0.11$ mm, $h = 2.90 \pm .26$ mm, $L_0c = 2.87 \pm 0.40$ mm for native rat trachea; $t = 0.38 \pm 0.12$ mm, $h = 3.18 \pm 0.16$ mm, $L_0t = 3.75 \pm 0.54$ mm for decellularized rat trachea; $t = 0.51 \pm 0.32$ mm, $h = 3.95 \pm 0/12$ mm, $L_0c = 7.51 \pm 0.28$ mm for engineered rat trachea.

Average and SD values of these three morphometric parameters for tension are $t = 0.60 \pm 0.09$ mm, $h = 2.99 \pm 0.46$ mm, $L_0t = 9.33 \pm 2.06$ mm for native monkey trachea; $t = 0.84$ mm, $h = 2.39 \pm 0.20$ mm, $L_0t = 5.74 \pm 2.24$ mm for engineered monkey trachea. Average and SD values of these three morphometric parameters for compression are $t = 0.64 \pm 0.05$ mm, $h = 9.15 \pm 2.44$ mm, $L_0c = 7.87 \pm 0.83$ mm for native monkey trachea; $t = 0.57 \pm 0.13$ mm, $h = 8.90 \pm 2.56$ mm, $L_0c = 7.43 \pm 0.46$ mm for engineered monkey trachea.

For tensile testing, rectangular specimens were glued to 1-mm sections of sand paper at each end of the tissue slices, and each end was affixed to grips, with tension along the long axis of the airway tissue. Tissues were then cyclically preconditioned for three cycles to 10% strain, and pulled until failure at a strain rate of 1-mm/min.

Nondestructive compression tests were performed on circular specimens by placing each sample between two compression plates fixed at the test machine grips, with the long axis of the airway perpendicular to the compression force direction. The specimens were compressed with a 3-mm/min strain rate until complete occlusion of the lumen.

Chick chorioallantoic membrane assay

Fertilized chicken eggs were incubated at 37°C and constant humidity. At 3 days of incubation, an oval window of ~ 3 mm in diameter was cut into the shell to reveal the embryo and chorioallantoic membrane (CAM) vessels. The window was sealed with tape and the eggs were returned to the incubator for a further 5 days. At day 8 of incubation, 4×4 mm acellular TSBT matrix or polyester (negative control) was placed on the CAM between branches of the blood vessels. About 10–12 eggs were utilized for each experimental condition. Samples were examined daily until 7 days after placement, wherein they were photographed *in ovo* with a stereomicroscope to quantify the blood vessels surrounding the sample. Blood vessels less than 10 μm in diameter converging toward the tissues were counted by blinded assessors with the mean of the counts being considered.

Rat implantation studies

Eleven rats (200–250 g, male and female, Fisher 344; Charles River, Inc., MA or Harlan Sprague Dawley, Inc., IN) were anesthetized using intraperitoneal injection of a mixture of ketamine (100 mg/kg) and xylazine (10 mg/kg). A midline cervical incision was performed from the level of the larynx to the suprasternal notch. The trachea was dissected along its entire length and freed of any associated tissue under observation of a microscope (Leica M125; Leica microsystems, IL). A three-ring segment of recipient trachea was removed. An 8-mm long, 4-mm diameter tissue-engineered trachea was placed into the defect and sutured as an interpositional end-to-end anastomosis with 8-0 monofilament sutures (Johnson & Johnson, NJ) using continuous stitches. The animal maintained ventilation through the tracheostomy without mechanical ventilatory support. Postoperatively, the rats were treated with meloxicam (0.3 mg/kg) in the drinking water for 48 h. This rat study was approved by the Yale University Institutional Animal Care and Use Committee.

Nonhuman primate implantation studies

Three old world monkeys (*Chlorocebus pygerythrus* or vervet monkeys, 3.3–5.5 kg) were implanted with engineered tracheas. The recipient monkeys were sedated with 8 mg/kg ketamine and the ventral neck was shaved. Buprenorphine (0.01 mg/kg, intradermal) was administered to provide preemptive analgesia, followed by endotracheal intubation and intravenous catheter placement. Propofol anesthesia was initiated with a 1.5 mL/kg IV bolus and followed by 1 mL/kg/h infusion. Under anesthesia, the monkey was placed in a supine position and the neck prepped and draped in a sterile manner and respirations sustained by ventilator to maintain end tidal carbon dioxide levels of 25–30. Thereafter, a small horizontal skin incision of 2.5–3.0 cm in length was made at the level of the suprasternal notch to expose the trachea, mobilizing and retracting ventral neck muscles, to free the segment of trachea to be excised. The recipient trachea was transected at the second ring below the epiglottis and three rings of tracheal segment were removed. A 18-mm long, 6-mm diameter TSBT was placed into the defect trachea. It was sutured starting with the distal anastomosis as an interpositional end-to-end anastomosis with 7-0 absorbable PDS II sutures (Johnson & Johnson, NJ) using continuous stitches. After tracheal graft fixation, the strap muscles were mobilized medially and used to cover the TSBT. The platysma layer was closed with simple interrupted 5.0 absorbable sutures, followed by closure of the skin incision with buried continuous 5.0 sutures. Upon completion of the surgery, the monkeys received meloxicam (0.2 mg/kg IM) and were continuously monitored during recovery from anesthesia and then at regular intervals over the first 24 h postsurgery, with attention to respiratory function and airway patency. The animals were euthanized at 2, 4, and 7 weeks, and the tracheal segment with the implanted tissue was explanted and fixed in 10% formalin for further analysis. All primate experimental and surgical procedures were approved by the Institutional Animal Care and Use Committee of the St. Kitts Biomedical Research Foundation.

Histological analysis

Explant samples comprising metal stents encased in tissue were fixed in 10% formalin and then embedded along with the metal stent in methylmethacrylate resin.[27] The anastomoses regions were separated and the rest of the sample encased in the stent was embedded in plastic resin. Thin sections were cut from the embedded samples and transferred onto slides. Hematoxylin and eosin (H&E), Mason's trichrome, Gomori, and Alcian blue staining were performed on the plastic-embedded sections after removal of the resin following regular histological techniques.[28] Images were obtained using an Axiovert

200 M microscope (Zeiss, Inc., NY) equipped with an AxioCam camera and AxioVision software.

Immunofluorescence staining

Luminal sections of the explants were separated with a scalpel after formalin fixation of the TSBTs and embedded into paraffin to enable immunostaining procedures. Thin 5-μm sections were processed by regular histological methods and then stained with antibodies for immunofluorescence detection of various markers. Sections were blocked for 1 h at room temperature (RT), stained with primary antibodies for 1 h at RT, or overnight at 4°C, washed with PBS, stained with secondary antibodies for 1 h at RT, washed with PBS, and then mounted with DAPI containing mounting medium. The following primary antibodies were utilized: E-cadherin (1:50, Cat#15148; Abcam), smooth muscle actin (SMA, 1:150, Cat#M0851; Dako), von Willebrand factor (vWF, 1:200, Cat#6994; Abcam), and cytokeratin 5 (CK5, 1:100, Cat# PA1-37974; Pierce). Alexa Fluor 555 goat anti-rabbit and goat anti-mouse dyes (Life Technologies, NY) were utilized at 1:500 as secondary antibodies. Samples were imaged with a Leica DS600 microscope and Leica Applications Suite software (Leica microsystems, IL).

Statistical analysis

The mechanical properties in terms of moduli are represented as mean ± SD. For the CAM assay, the number of blood vessels is presented as the mean ± SEM. Statistical significance was evaluated by using the unpaired Students t-test. A p value of less than 0.05 was considered to be significant.

Results

Creation of an engineered tissue–stent composite (TSBT) as a tracheal replacement

We first prepared a scaffold by wrapping degradable, biocompatible PGA mesh around clinical-grade nitinol stents (Fig. 1A, B). Primary vascular SMCs (rat, bovine, or human origin) are seeded onto sterilized PGA–stent scaffolds, and are grown in culture medium that is designed to support the replication of and collagenous matrix synthesis by SMCs, as previously reported.[3,20,22] After 8 weeks, the PGA scaffold has largely degraded, resulting in a tubular SMC-based tissue that completely encases the stent, resulting in a tissue–stent composite (Fig. 1C, D). Thorough decellularization using detergents and high ionic strength salts[20,24,25] results in quantitative cellular removal (Fig. 1E) while retaining the integrity of the extracellular matrix proteins. These final TSBTs are acellular and hence largely devoid of immunogenic material. The acellular matrix has been shown to maintain its mechanical characteristics at 4°C for up to 6 months.[22,24] Such a method is versatile and can be utilized to produce TSBTs in diameters ranging from 4 to 16 mm (sizes suitable for rodents and humans, respectively, Fig. 1E, F).

Biochemical and histological characterization of TSBTs

Histology of TSBTs revealed that no nuclei remains in the matrix after decellularization (Supplementary Fig. S1a, b and Fig. 6A, D; Supplementary Data are available online at www.liebertpub.com/tea). The decellularized matrix itself is primarily composed of collagen, confirmed by Gomori's staining (green, Supplementary Fig. S1c, d). Alcian blue staining reveals low levels of GAGs throughout the matrix (Supplementary Fig. S1a, b). We quantified the collagen content using the hydroxyproline assay. The TSBT scaffold (neglecting the nitinol stent) contains equivalent collagen, as a fraction of dry weight, when compared with native rat tracheal matrix. In contrast, native rat matrix that was decellularized had less than half the collagen content (Fig. 2A, $p = 0.0027$ when compared with native rat trachea). The TSBT matrix was also analyzed by the Blyscan assay for sGAG content. When compared with native rat tracheal matrix, both native decellularized matrix and the TSBT matrix

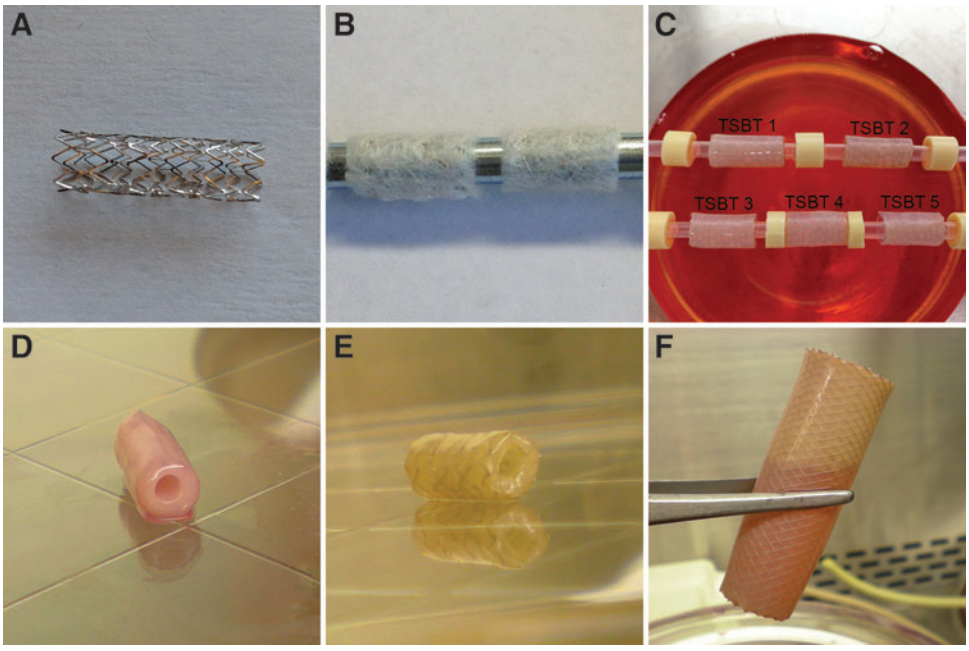

FIG. 1. Creation of the engineered TSBT. **(A)** Clinical-grade metal nitinol stent, 6 mm diameter. **(B)** Stent–polymer (polyglycolic acid) composite scaffold. **(C)** Bioreactor culture of smooth muscle cells on stent–polymer scaffold. **(D)** Engineered cellular tissue–stent composite at the end of 8 weeks. **(E)** Final product for tracheal replacement—4-mm diameter decellularized engineered TSBT. **(F)** Gross picture of a 16-mm diameter TSBT, of a size suitable for clinical airway repair. TSBT, tissue–stent biocomposite trachea.

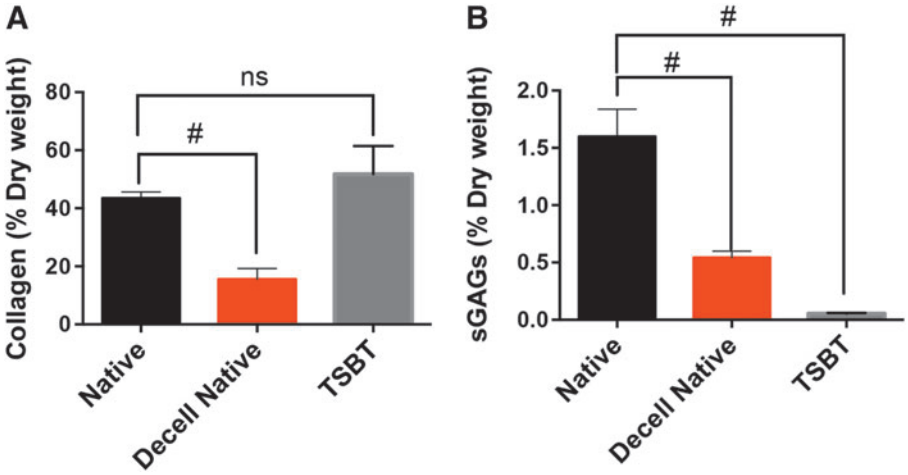

FIG. 2. Biochemical characterization of engineered TSBTs. **(A)** Collagen quantified by hydroxyproline assay for native rat, decellularized native rat trachea, and TSBTs. **(B)** sGAGs quantified by Blyscan assay for native rat trachea, decellularized native rat trachea, and TSBT. ns, not significant; $^{\#}p < 0.01$ ($n = 4$ for native rat trachea, $n = 3$ for decellularized native rat trachea, $n = 3$ for TSBT). sGAGs, sulfated glycosaminoglycans.

contained significantly lower quantities of sGAGs (Fig. 2B, $p < 0.01$). This likely reflects the efficient removal of hydrophilic GAG molecules from the extracellular matrix, as well as removal of cellular GAG constituents, by the decellularization process.

Angiogenic properties of TSBT matrix

To test the angiogenic properties of the TSBT acellular matrix, the CAM assay was performed.[24,29] TSBT implants were compared against nylon negative control, as well as nylon membrane loaded with 200 ng/mL of vascular endothelial growth factor (VEGF). After 7 days of incubation, there was a visual increase in the number of blood vessels converging toward the TSBT matrix material as compared with nylon control samples (Fig. 3A). (A small portion of the TSBT scaffold has been enlarged to clearly reveal the vessels converging into the matrix.) Quantification of number of vessels at 7 days revealed that the TSBT matrix had a stronger angiogenic effect than did a nylon membrane

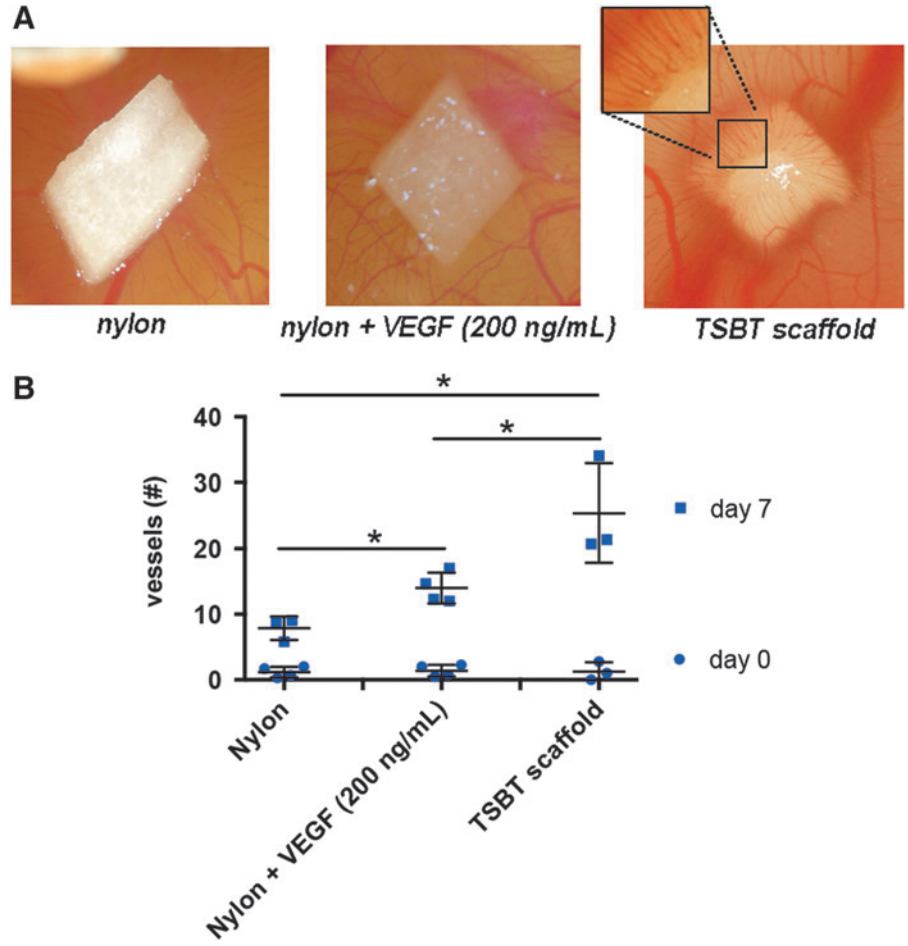

FIG. 3. Angiogenic testing of TSBTs: chorioallantoic membrane assay. **(A)** Representative images of negative control (nylon membrane), nylon loaded with VEGF 200 ng/mL and engineered matrix scaffold TSBT placed *in ovo* at the end of 7 days of incubation. **(B)** Number of vessels attracted toward the matrices at days 0 and 7 post-implantation, significant differences between all groups at day 7. $^{*}p < 0.05$ (day 0: $n = 4$ for nylon, $n = 4$ for nylon + VEGF, $n = 3$ for TSBT scaffold; day 7: $n = 3$ for nylon, $n = 4$ for nylon + VEGF, $n = 3$ for TSBT scaffold). VEGF, vascular endothelial growth factor.

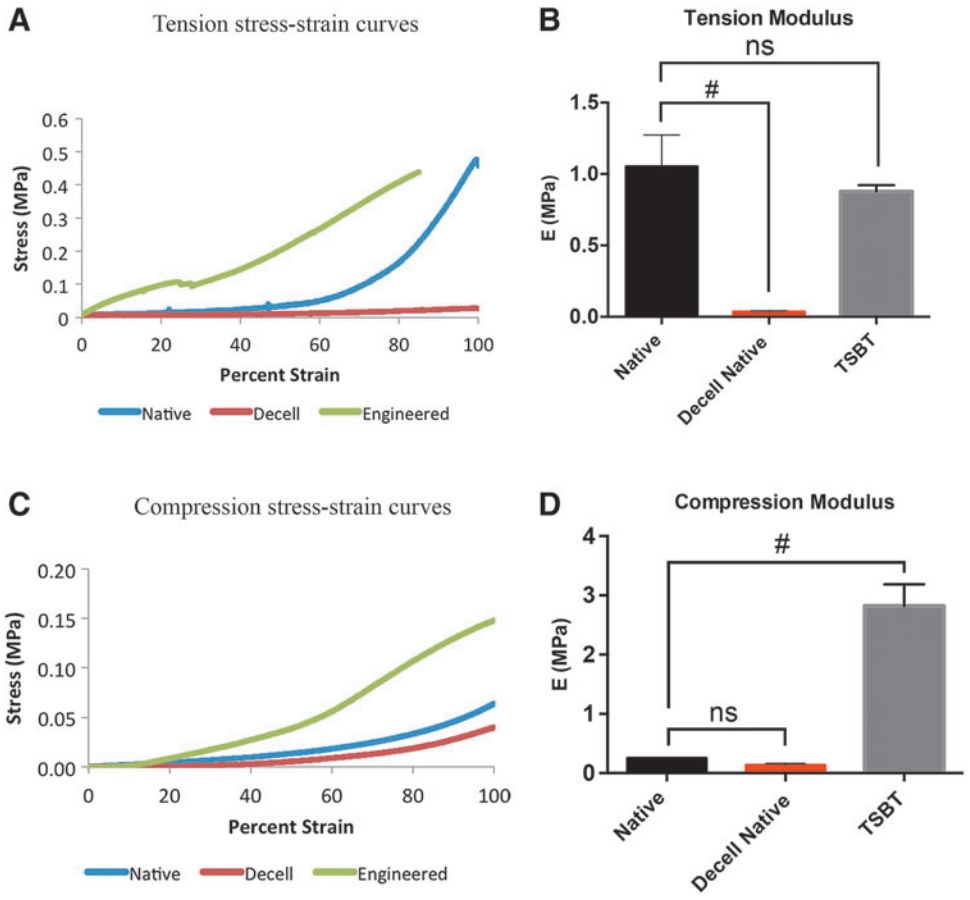

FIG. 4. Mechanical characterization of 4-mm diameter TSBTs and rat tracheas: **(A, C)** Representative stress–strain curves for tensile **(A)** and compressive **(C)** loads comparing TSBT (*green curve*) with native (*blue*) and decellularized native (*red*) rat tracheas. Tensile and compressive moduli for TSBT and rat trachea are shown in **(B)** and **(D)**, respectively. Moduli computed from slope of curves beyond 60% strain. For tensile and compression studies, $n=3$ for all samples. # denotes $p<0.05$.

loaded with 200 ng/mL of VEGF (Fig. 3B, $p<0.05$). These results suggest that the TSBT matrix has the potential to stimulate formation of microvasculature *in vivo.*

Mechanical properties of TSBTs

We compared the tensile and compressive bulk properties of 4-mm diameter TSBTs against those of native and decellularized rat tracheal tissues (Fig. 4). Typical stress–strain curves in tension (Fig. 4A) and compression (Fig. 4C) are shown. Evaluating modulus at the linear portions of the stress–strain curves, beyond 60% strain, showed that 4-mm diameter TSBTs and native rat trachea had similar tensile properties, whereas decellularized rat trachea was significantly weaker than the TSBT (Fig. 4B) ($n=3$ for all samples). In compression, the TSBTs were significantly stiffer than both the native and the decellularized rat tracheas (Fig. 4D, $n=3$ for all samples), implying that the TSBT constructs would resist collapse under physiological forces *in vivo*.

In addition, the mechanical properties of 6-mm diameter TSBTs were compared with those of native primate (vervet monkey, 6-mm diameter) tracheas (Supplementary Fig. S2, stress–strain curves shown in panels ''a'' and ''c''). Tensile moduli (measured at the linear portion of the stress–strain curve beyond 60% strain) were 1.5 ± 0.1 MPa ($n=4$) for native primate tracheas and 2.4 ± 0.7 MPa ($n=3$) for TSBTs (Supplementary Fig. S2a, b). Compressive moduli (also measured beyond 60% strain) were 0.14 ± 0.01 MPa ($n=3$) and 2.40 ± 0.05 MPa ($n=2$) for native primate trachea and TSBTs, respectively (Supplementary Fig. S2c, d).[24,25,30]

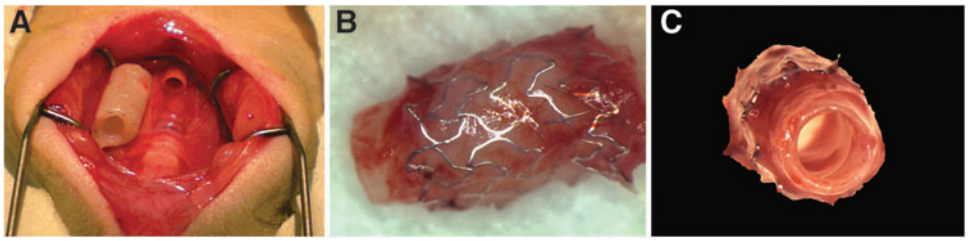

FIG. 5. *In vivo* testing of TSBT in a rat model. **(A)** End-to-end implantation of a 4-mm TSBT as a tracheal replacement. **(B)** Explant at 8 weeks showing metal stents and remodeled tissue with new angiogenic ingrowth. **(C)** Luminal view of explant at 8 weeks showing a patent graft.

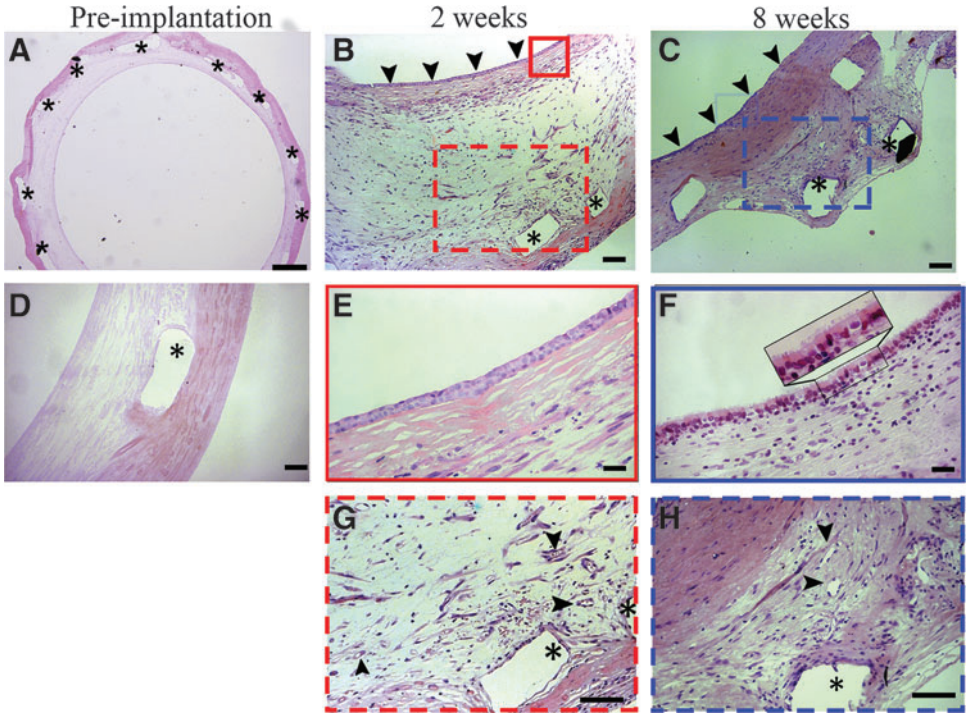

FIG. 6. Remodeling of TSBT in a rat model over 8 weeks. H&E staining of a preimplant TSBT indicating acellular nature of graft **(A, D)**. Remodeled with cellular infiltration throughout at weeks 2 and 8 postimplant **(B, C)**. Arrowheads in **(B, C)** indicate luminal surface of TSBTs. Luminal cell repopulation at 2 weeks shows cuboidal cells **(E**, enlarged *solid red box* from **B)** and at 8 weeks shows ciliated cells **(F**, enlarged *solid blue box* from **C)**. Repopulation of the TSBT walls shows areas that appear to be vascularized developed at 2 weeks **(G**, enlarged *dotted red box* from **B)**, and at 8 weeks **(H**, enlarged *dotted blue box* from **C)**. *Arrowheads* in **(G, H)** indicate microvessels. *Asterisk* (*) indicates location of metal stent struts. Scale bars: **(A)**, 500 μm; **(B–D)**, 100 μm; **(E, F)**, 25 μm; **(G, H)**, 100 μm. H&E, hematoxylin and eosin.

Similar to findings with comparison to rat airway tissues, the tensile moduli were similar between 6-mm TSBTs and native primate tracheas, but TSBTs showed higher compressive moduli than the native primate tracheas.

In vivo *testing of TSBTs in a rat model*

To test the ability of TSBTs to replace the airway, we first implanted TSBTs in a rat model ($n = 11$). Rat tracheal grafts were 4 mm in diameter and 8 mm in length. For all implantations, a segment of native trachea corresponding to the length of the engineered TSBT was excised, and then the TSBT was anastomosed in an end-to-end manner (Fig. 5). No postoperative antibiotics were administrated. Tracheas were explanted at varying times ranging from 1 to 8 weeks. At the end of 8 weeks, the explants were well healed and patent and showed signs of angiogenesis (Fig. 5B, C)

Histological analysis revealed progressive host cell repopulation of the TSBT matrix over time (Fig. 6A–C), which proceeded from both the luminal and abluminal surfaces (arrowheads in Fig. 6B, C show luminal surface). The matrix was essentially completely repopulated with host cells after 8 weeks (Fig. 6C). (Identity of all samples as being TSBT implant, rather than native trachea, was confirmed in all cases by the presence of tissue voids where stent struts resided, indicated by ''*'' symbols.) Progressive epithelial remodeling on the lumen was observed over a period from 2 to 8 weeks. Cuboidal cells (Fig. 6B, E) were visible on the TSBT lumen at 2 weeks. In certain samples, we also observed squamous luminal epithelium (data not shown). By 8 weeks, ciliated epithelium on the lumen (Fig. 6C, F) was observed. Microvasculature was

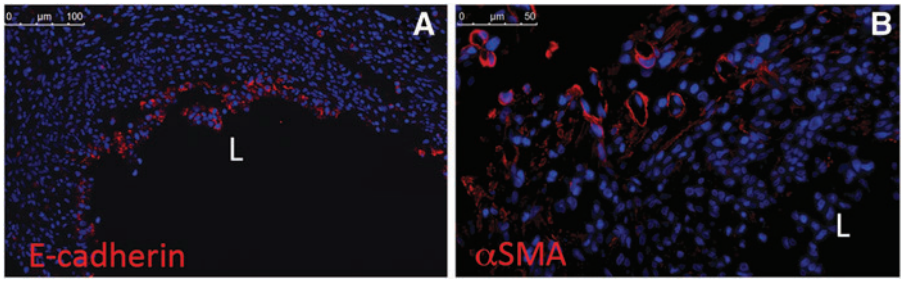

FIG. 7. Immunofluorescence of remodeled TSBT in a rat model at 1 week. Immunofluoresence staining for **(A)** E-cadherin (*red*), a pan-epithelial marker and **(B)** Alpha smooth muscle actin (*red*), a marker for smooth muscle cells. Scale bar: **(A)**, 100 μm; **(B)**, 50 μm. L, lumen of TSBT.

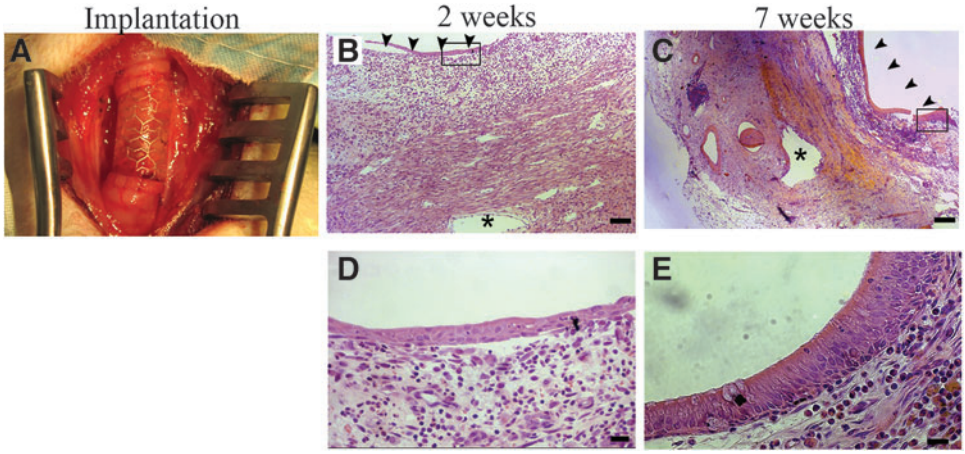

FIG. 8. *In vivo* testing of TSBT in a primate model **(A)** Remodeling over 7 weeks. Low power H&E staining of TSBT in a nonhuman primate showing cross section of TSBT wall at **(B)** 2 weeks and **(C)** 7 weeks. *Asterisk* (*) indicate stent struts, *arrowheads* point to luminal surface. H&E of TSBT shows a simple cuboidal epithelium at **(D)** 2 weeks and multilayer pseudostratified columnar luminal cells at 7 weeks in primate explants **(E)**. Scale bars: **(B, C)**, 100 μm; **(D, E)**, 20 μm.

observed in the remodeled TSBT as early as 2 weeks (arrowheads, Fig. 6G) and persisted at 7 weeks (arrowheads in Fig. 6H). No evidence of neocartilage formation or calcification was detected in explanted samples.

For evaluation of the identity of repopulating cells, we utilized immunofluoresence staining for epithelium and vasculature of 1 week explants. Immunofluorescence of paraffin-embedded rat explants revealed E-cadherin staining (Fig. 7A) restricted to the lumen of the explant, thus confirming the repopulation with cells of an epithelial phenotype in the lumen. Alpha SMA (αSMA)-positive cells (Fig. 7B) were detected in the outer layers of the explant, in circular forms, indicative of microvascularization of the TSBT.

In vivo *testing of TSBTs in a nonhuman primate model*

TSBTs were implanted in vervet monkeys ($n=3$, Fig. 8A) similar to the rat implants. Grafts were created to match primate trachea luminal dimensions, which measured 6 mm diameter and 1.8 cm in length. For primate implantations at 2, 4, and 7 weeks, all grafts were patent at the time of explant. The TSBT was progressively epithelialized on the lumen from a simple cuboidal cell layer at 2 weeks (Fig. 8B, D) to a multilayer pseudostratified columnar epithelium at 7 weeks (Fig. 8C, E. Arrowheads in Figure 8B and C indicate luminal surface, ''*'' indicates stent strut locations). Indeed, pseudostratified cells at 7 weeks had an appearance quite similar to that of native vervet tracheal epithelium.

We assessed the phenotype of the remodeled luminal cells using immunofluorescence at 7 weeks. E-cadherin staining (Fig. 9A, C) confirmed the epithelial nature of the luminal lining. Staining for cytokeratin 5 (CK5, Fig. 9B, D), an intermediate filament protein and a marker for basal cells in the large airways,[30,31] provided evidence of basal-like cells localized to the base of the luminal cell layer. In certain other areas, CK5 staining was positive throughout the newly formed epithelium (data not shown) similar to a more metaplastic epithelial layer that is observed after injury of the native airway.[29,32,33] In addition, primate implants at 7 weeks positively stain for the presence of goblet cells (Supplementary Fig. S3C, D). These results imply that host-derived basal-like cells,

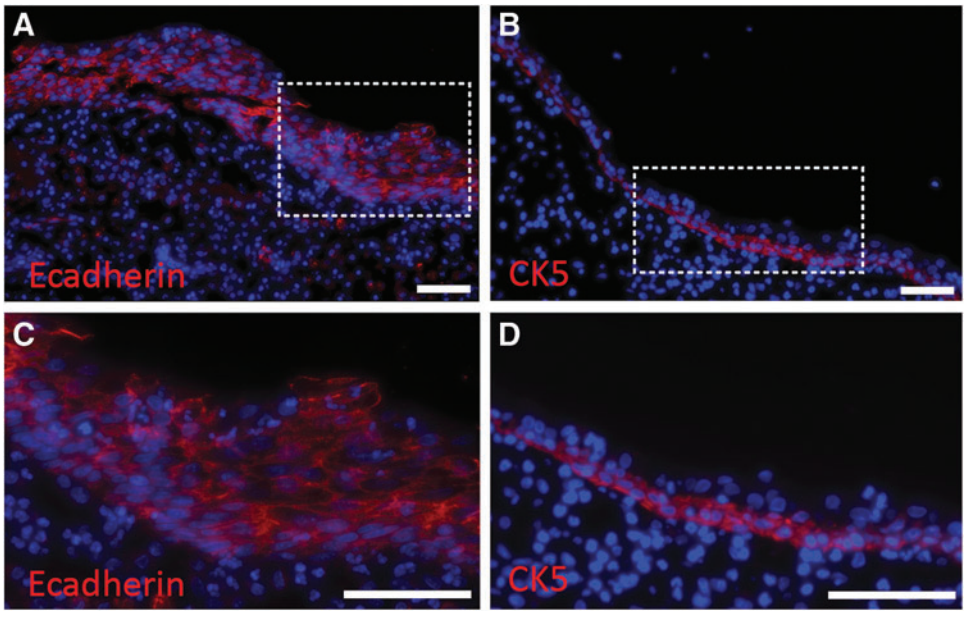

FIG. 9. Immunofluorescence of remodeled TSBT in a primate model at 7 weeks. Immunofluoresence staining for **(A, C)** E-cadherin (*red*), a pan-epithelial marker and for **(B, D)** cytokeratin5 (*red*), a marker for basal-like cells. CK5 staining observed at the base of the luminal cell layer. DAPI-stained nuclei are *blue*. **(C)** is enlarged from *dotted area* in **(A)**; **(D)** is enlarged from *dotted area* in **(B)**. Scale bars: **(A–D)** 75 μm.

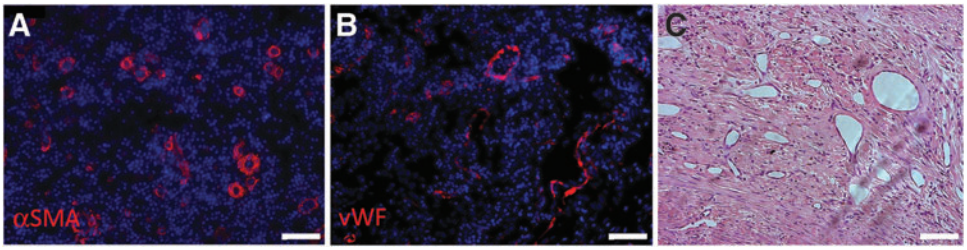

FIG. 10. Microvessels formed in remodeled TSBT at 7 weeks in a primate model. **(A)** αSMA (*red*) positive and **(B)** vWF (*red*) positive cells lining microvascular structures of the remodeled TSBT. Nuclei in **(A, B)** are *blue*. **(C)** H&E staining of remodeled wall of TSBT from a primate showing vascular structures. Scale bars: **(A–C)** 75 μm. αSMA, alpha smooth muscle actin; vWF, von Willebrand factor.

which are CK5+, migrate onto the implanted acellular graft lumen and, over time, repopulate the graft with autologous epithelium. This potential process of basal cell-derived epithelial repopulation is similar to that observed in various disease models of airway and lung regeneration *in vivo*[13,31,34]

Neovascularization was also observed in primates in response to the TSBT, similar to the rat implantation studies. αSMA (Fig. 10A) as well as vWF (Fig. 10B), indicative of SMCs and endothelial cells, respectively, were observed in remodeled TSBT walls. In many cases, microvascular structures were also visible by H&E (Fig. 10C). Active remodeling of the implanted collagenous TSBT matrix was observed by Trichrome staining of primate explants at 7 weeks. Collagen was localized around newly formed vascular structures (Supplementary Fig. S4b), and collagen fiber formation was detected in the outer layers of the explant (Supplementary Fig. S4a). Overall, these results are indicative of an active remodeling of the TSBT, with formation of layers resembling an inner luminal epithelium, and an outer connective tissue-like layer.

Patency of TSBTs

Overall patency (defined as functional ventilation at the planned endpoint) was 60% in the small animal rat model ($n=11$) and 100% in the nonhuman primate model ($n=3$) (Table 1). All animals tolerated grafting well, with no evidence of perforation, stent migration, or stent erosion into adjacent tissues. There was also no evidence of graft collapse in any case, and no stenting was required in any animal. There were no instances of graft infection. Grafts integrated well at the anastomotic sites at all explant times. Importantly, because the TSBT is nonliving, it did not require vascular perfusion to prevent cellular hypoxia, so no ''prevascularization'' was performed for any of the TSBT implantations.

However, in 4 of 11 cases of rat implantation, we observed stenosis at time points varying from 2 to 6 weeks (Supplementary Fig. S5). In such cases, there was a little to no epithelial cell repopulation of the tracheal lumen, but an abundance of connective tissue that encroached on the airway (Supplementary Fig. S5b, c). These results suggest that an accelerated rate of luminal epithelialization may retard stenosis of the TSBT. This hypothesis remains to be tested in future studies.

Table 1. Summary of *In Vivo* Testing of Tissue–Stent Biocomposite Tracheas

Animal model	*Implant times*	*Outcome*
Rats, $n=7$	1, 1, 1, 2, 2, 8, 8	Patent
Rats, $n=4$	2, 2, 3, 6	Stenosis
Primate, $n=3$	2, 4, 7	Patent

Discussion

Current advances in tracheal engineering have shown limited success and overall there is a pressing need for alternative approaches. The design reported here is, to our knowledge, a unique approach to producing a functional tracheal substitute. We have focused our design on the following key criteria: (1) provide an appropriate biomechanical construct to prevent airway collapse, since this has plagued previous studies of decellularized airway replacement[10,20]; (2) support rapid vascularization of the implanted scaffold to decrease risk of graft infection and perforation; (3) avoid the use of patient's cells, so that no invasive biopsies or cell culture ''wait time'' is necessary before graft implantation; (4) avoid immunosuppressive treatment by providing an acellular construct; and (5) provide an implant that has mechanical properties similar to native trachea, thereby providing ease of surgical handling.[2]

Previous tracheal replacements have focused on decellularization of native airways,[8,9,20,32,33] or on entirely synthetic substrates that are seeded with autologous cells.[3] However, human and animal studies have shown that both approaches have significant limitations. Decellularization of native airways causes cartilagenous rings to lose their inherent stenting function, since cell and GAG removal from cartilage results in loss of compressive modulus. This has led to repeated requirements for stenting to maintain airway patency of decellularized tracheas.[24] In contrast, purely synthetic materials may confer adequate stiffness, but suffer from inadequate integration into host airways, minimal angiogenic stimulus, a propensity for infection, and can require many months for appreciable host cell repopulation.[24,25] The TSBT described herein resolves these limitations, since the indwelling stent prevents airway collapse, whereas the decellularized matrix promotes angiogenesis and allows rapid remodeling by host cells.

We utilized nitinol stents to provide mechanical strength to the TSBTs. Nitinol stents have been utilized previously in the clinic to prevent airway obstruction and in some cases are considered superior to other stents.[35] A comparison of the mechanical properties of the TSBTs with those of the native

primate trachea revealed similar tensile properties, and TSBTs had a higher compressive modulus than native airways. The high compressive modulus was conferred by the nitinol stenting component of the TSBT. Consistent with the good compressive modulus, we did not observe any stent-related complications such as airway collapse or stent migration into peritracheal tissues. Other investigators have tested polypropylene[36] or silicone[37] stents as part of artificial tracheal constructs, with varying degrees of success. Future efforts to tailor the properties of the stent to more closely match the compressive properties of the native trachea may further enhance host remodeling responses, and potentially decrease any propensity to fibrotic stenosis that was observed in some animals.

Although some groups have utilized collagen coatings on stents as tracheal replacements,[38,39] problems related to stent material exposure, perforation, and ulcers have been reported. We did not observe such problems in our studies, perhaps because the tissue encasing this stent is mature, cross-linked collagenous matrix as opposed to a solubilized collagen coating. Because the TSBT matrix is proangiogenic as demonstrated by the CAM assays, the graft is rapidly vascularized *in vivo*. This may impart a resistance to infection and perforation. Rapid revascularization may additionally accelerate the re-epithelialization process, with cell migration and basal cell infiltration from the sites of anastomosis.[28] In the TSBT, regeneration of epithelium appears to evolve from squamous to cuboidal to pseudostratified cells over time.[40,41] Such progressive regeneration of the epithelium is similar to that observed by other investigators after epithelial injury.[42,43]

Although the TSBTs functioned well overall as tracheal replacements, there still persist some confounding observations. Of the 11 rats in the animal study, we observed 4 cases of failure because of stenosis. Various prior studies have highlighted the important role of the epithelium in preventing stenosis after airway injury, which is likely mediated by fibroblasts and macrophage activation.[33,41,44,45] Delayed epithelialization could play a role in our observations of occasional stenosis, since no epithelial lining was observed in cases where we observed airway narrowing. It remains to be investigated whether luminal coating of the TSBT with autologous epithelium or basal cells before implantation could speed epithelialization and decrease stenosis *in vivo*.

Overall, our findings are the first to show that a tissue-engineered, acellular graft can regenerate into a functional, vascularized, epithelialized airway. Because the size and shape of the engineered trachea are dictated by the dimensions of the nondegradable stents that are used for culture, TSBTs can be scaled easily to create tracheal replacements of arbitrary diameters and lengths. Hence, the TSBT warrants further study as a novel, off-the-shelf alternative for tracheal replacement.

Acknowledgments

We sincerely thank Dr. Nancy Troiano and Rose Webb at the Yale Orthopedic histology and histomorphometry laboratory for help with resin embedding techniques. This work was funded by NIH grant 1U01HL111016-03 (L.E.N), T32GM086287 (L.E.N.). P.D.C and L.U. are supported by NIHR. S.S. is supported by CT Stem Cell grant (S01515).

Author Contributions

L.Z., S.S., and A.V.L. performed experiments, data analysis, figure preparation, and article writing. A.H.H., P.M., A.B., and P.D.C. performed experiments and data analysis. G.H., A.B., and T.Y. performed surgical procedures. J.Z. and M.G.C. performed surgical procedures and article writing. K.L., A.G., M.H.K., L.G., K.A.R., A.S., and E.C. performed experiments. A.G. performed experiments and figure preparation. L.U. performed experiments and data analysis, figure preparation, and article writing. L.E.N. gave idea and conceptualization, performed data analysis, figure preparation, article writing, overseeing entire project, funding source, and is the corresponding author.

Disclosure Statement

L.E.N. is a founder and shareholder in Humacyte, Inc., which is a regenerative medicine company. Humacyte produces engineered blood vessels from allogeneic SMCs for vascular surgery. L.E.N.'s spouse has equity in Humacyte, and L.E.N. serves on Humacyte's Board of Directors. L.E.N. is an inventor on patents that are licensed to Humacyte and that produce royalties for L.E.N. L.E.N. has received an unrestricted research gift to support research in her laboratory at Yale. Humacyte did not fund this study and did not influence the conduct, description, or interpretation of the findings in this report.

References

1. Del Gaudio, C., Baiguera, S., Ajalloueian, F., Bianco, A., and Macchiarini, P. Are synthetic scaffolds suitable for the development of clinical tissue-engineered tubular organs? J Biomed Mater Res A **102,** 2427, 2014.
2. Rich, J.T., and Gullane, P.J. Current concepts in tracheal reconstruction. Curr Opin Otolaryngol Head Neck Surg **20,** 246, 2012.
3. Jungebluth, P., Alici, E., Baiguera, S., Le Blanc, K., Blomberg, P., Bozóky, B., Crowley, C., Einarsson, O., Grinnemo, K.-H., Gudbjartsson, T., Le Guyader, S., Henriksson, G., Hermanson, O., Juto, J.E., Leidner, B., Lilja, T., Liska, J., Luedde, T., Lundin, V., Moll, G., Nilsson, B., Roderburg, C., Strömblad, S., Sutlu, T., Teixeira, A.I., Watz, E., Seifalian, A., and Macchiarini, P. Tracheobronchial transplantation with a stem-cell-seeded bioartificial nanocomposite: a proof-of-concept study. Lancet **378,** 1997, 2011.
4. Delaere, P., Vranckx, J., Verleden, G., De Leyn, P., Van Raemdonck, D., and Leuven Tracheal Transplant Group. Tracheal allotransplantation after withdrawal of immunosuppressive therapy. N Engl J Med **362,** 138, 2010.
5. Delaere, P.R., Vranckx, J.J., Den Hondt, M., and Leuven Tracheal Transplant Group. Tracheal allograft after withdrawal of immunosuppressive therapy. N Engl J Med **370,** 1568, 2014.
6. Nomoto, M., Nomoto, Y., Tada, Y., Tani, A., Otsuki, K., Suzuki, R., Nakamura, T., and Omori, K. Bioengineered trachea using autologous chondrocytes for regeneration of tracheal cartilage in a rabbit model. Laryngoscope **123,** 2195, 2013.
7. Fabre, D., Kolb, F., Fadel, E., Mercier, O., Mussot, S., Le Chevalier, T., and Dartevelle, P. Successful tracheal replacement in humans using autologous tissues: an 8-year experience. Ann Thorac Surg **96,** 1146, 2013.

8. Baiguera, S., Jungebluth, P., Burns, A., Mavilia, C., Haag, J., De Coppi, P., and Macchiarini, P. Tissue engineered human tracheas for in vivo implantation. Biomaterials **31,** 8931, 2010.
9. Macchiarini, P., Jungebluth, P., Go, T., Asnaghi, M.A., Rees, L.E., Cogan, T.A., Dodson, A., Martorell, J., Bellini, S., Parnigotto, P.P., Dickinson, S.C., Hollander, A.P., Mantero, S., Conconi, M.T., and Birchall, M.A. Clinical transplantation of a tissue-engineered airway. Lancet **372,** 2023, 2008.
10. Gonfiotti, A., Jaus, M.O., Barale, D., Baiguera, S., Comin, C., Lavorini, F., Fontana, G., Sibila, O., Rombolà, G., Jungebluth, P., and Macchiarini, P. The first tissue-engineered airway transplantation: 5-year follow-up results. Lancet **383,** 238, 2014.
11. Trabelsi, O., del Palomar, A.P., López-Villalobos, J.L., Ginel, A., and Doblaré, M. Experimental characterization and constitutive modeling of the mechanical behavior of the human trachea. Med Eng Phys **32,** 76, 2010.
12. Teng, Z., Trabelsi, O., Ochoa, I., He, J., Gillard, J.H., and Doblare, M. Anisotropic material behaviours of soft tissues in human trachea: an experimental study. J Biomech **45,** 1717, 2012.
13. Rock, J.R., Onaitis, M.W., Rawlins, E.L., Lu, Y., Clark, C.P., Xue, Y., Randell, S.H., and Hogan, B.L.M. Basal cells as stem cells of the mouse trachea and human airway epithelium. Proc Natl Acad Sci U S A **106,** 12771, 2009.
14. Roomans, G.M. Tissue engineering and the use of stem/progenitor cells for airway epithelium repair. Eur Cell Mater **19,** 284, 2010.
15. Grillo, H.C. Tracheal replacement: a critical review. Ann Thorac Surg **73,** 1995, 2002.
16. Martinod, E. Airway transplantation using aortic allografts: a 'hot topic'. Eur J Cardiothorac Surg **41,** 1409, 2012.
17. Klepetko, W., Marta, G.M., Wisser, W., Melis, E., Kocher, A., Seebacher, G., Aigner, C., and Mazhar, S. Heterotopic tracheal transplantation with omentum wrapping in the abdominal position preserves functional and structural integrity of a human tracheal allograft. J Thorac Cardiovasc Surg **127,** 862, 2004.
18. Jungebluth, P., and Macchiarini, P. Airway transplantation. Thorac Surg Clin **24,** 97, 2014.
19. Delaere, P.R., and Van Raemdonck, D. The trachea: the first tissue-engineered organ? J Thorac Cardiovasc Surg **147,** 1128, 2014.
20. Elliott, M.J., De Coppi, P., Speggiorin, S., Roebuck, D., Butler, C.R., Samuel, E., Crowley, C., McLaren, C., Fierens, A., Vondrys, D., Cochrane, L., Jephson, C., Janes, S., Beaumont, N.J., Cogan, T., Bader, A., Seifalian, A.M., Hsuan, J.J., Lowdell, M.W., and Birchall, M.A. Stem-cell-based, tissue engineered tracheal replacement in a child: a 2-year follow-up study. Lancet **380,** 994, 2012.
21. Quint, C., Arief, M., Muto, A., Dardik, A., and Niklason, L.E. Allogeneic human tissue-engineered blood vessel. J Vasc Surg **55,** 790, 2012.
22. Niklason, L.E., Gao, J., Abbott, W.M., Hirschi, K.K., Houser, S., Marini, R., and Langer, R. Functional arteries grown in vitro. Science **284,** 489, 1999.
23. Niklason, L.E., Abbott, W., Gao, J., Klagges, B., Hirschi, K.K., Ulubayram, K., Conroy, N., Jones, R., Vasanawala, A., Sanzgiri, S., and Langer, R. Morphologic and mechanical characteristics of engineered bovine arteries. J Vasc Surg **33,** 628, 2001.
24. Dahl, S.L.M., Kypson, A.P., Lawson, J.H., Blum, J.L., Strader, J.T., Li, Y., Manson, R.J., Tente, W.E., Dibernardo, L., Hensley, M.T., Carter, R., Williams, T.P., Prichard, H.L., Dey, M.S., Begelman, K.G., and Niklason, L.E. Readily available tissue-engineered vascular grafts. Sci Transl Med **3,** 68ra9, 2011.
25. Quint, C., Kondo, Y., Manson, R.J., Lawson, J.H., Dardik, A., and Niklason, L.E. Decellularized tissue-engineered blood vessel as an arterial conduit. Proc Natl Acad Sci U S A **108,** 9214, 2011.
26. Grant, R.A. Estimation of hydroxyproline by the autoanalyser. J Clin Pathol **17,** 685, 1964.
27. Rippstein, P., Black, M.K., Boivin, M., Veinot, J.P., Ma, X.L., Chen, Y.X., Human, P., Zilla, P., and O'Brien, E.R. Comparison of processing and sectioning methodologies for arteries containing metallic stents, J Histochem Cytochem **54,** 673, 2006.
28. Kacena, M.A., Troiano, N.W., Wilson, K.M., Coady, C.E., and Horowitz, M.C. Evaluation of two different methylmethacrylate processing, infiltration, and embedding techniques on the histological, histochemical, and immunohistochemical analysis of murine bone specimens. J Histotechnol **27,** 119, 2004.
29. Fishman, J.M., Lowdell, M.W., Urbani, L., Ansari, T., Burns, A.J., Turmaine, M., North, J., Sibbons, P., Seifalian, A.M., Wood, K.J., Birchall, M.A., and De Coppi, P. Immunomodulatory effect of a decellularized skeletal muscle scaffold in a discordant xenotransplantation model. Proc Natl Acad Sci U S A **110,** 14360, 2013.
30. Cozzi, B., Bagnoli, P., Acocella, F., and Costantino, M.L. Structure and biomechanical properties of the trachea of the striped dolphin Stenella coeruleoalba: evidence for evolutionary adaptations to diving. Anat Rec A Discov Mol Cell Evol Biol **284,** 500, 2005.
31. Cole, B.B., Smith, R.W., Jenkins, K.M., Graham, B.B., Reynolds, P.R., and Reynolds, S.D. Tracheal Basal cells: a facultative progenitor cell pool. Am J Pathol **177,** 362, 2010.
32. Ghosh, M., Ahmad, S., Jian, A., Li, B., Smith, R.W., Helm, K.M., Seibold, M.A., Groshong, S.D., White, C.W., and Reynolds, S.D. Human tracheobronchial basal cells. Normal versus remodeling/repairing phenotypes in vivo and in vitro. Am J Respir Cell Mol Biol **49,** 1127, 2013.
33. Musah, S., Chen, J., and Hoyle, G.W. Repair of tracheal epithelium by basal cells after chlorine-induced injury. Respir Res **13,** 107, 2012.
34. Zuo, W., Zhang, T., Wu, D.Z., Guan, S.P., Liew, A.-A., Yamamoto, Y., Wang, X., Lim, S.J., Vincent, M., Lessard, M., Crum, C.P., Xian, W., and McKeon, F. p63(+)Krt5(+) distal airway stem cells are essential for lung regeneration. Nature **517,** 616, 2015.
35. Siegel, B., Bent, J.P., and Ward, R.F. Endotracheal nitinol stents: lessons from the learning curve. Otolaryngol Head Neck Surg **148,** 671, 2013.
36. Teramachi, M., Kiyotani, T., Takimoto, Y., Nakamura, T., and Shimizu, Y. A new porous tracheal prosthesis sealed with collagen sponge. ASAIO J **41,** M306, 1995.
37. Tsukada, H., Gangadharan, S., Garland, R., Herth, F., DeCamp, M., and Ernst, A. Tracheal replacement with a bioabsorbable scaffold in sheep. Ann Thorac Surg **90,** 1793, 2010.
38. Nakamura, T., Sato, T., Araki, M., Ichihara, S., Nakada, A., Yoshitani, M., Itoi, S.-I., Yamashita, M., Kanemaru, S.-I., Omori, K., Hori, Y., Endo, K., Inada, Y., and Hayakawa, K. In situ tissue engineering for tracheal reconstruction using a luminar remodeling type of artificial trachea. J Thorac Cardiovasc Surg **138,** 811, 2009.
39. Sekine, T., Nakamura, T., Liu, Y., Ueda, H., Matsumoto, K., and Shimizu, Y. Collagen coated Y-shaped prosthesis

for carinal replacement promotes regeneration of the tracheal epithelium. ASAIO J **46,** 421, 2000.
40. Wilhelm, D.L. Regeneration of tracheal epithelium. J Pathol Bacteriol **65,** 543, 1953.
41. Genden, E.M., Iskander, A., Bromberg, J.S., and Mayer, L. The kinetics and pattern of tracheal allograft re-epithelialization. Am J Respir Cell Mol Biol **28,** 673, 2003.
42. Nomoto, Y., Suzuki, T., Tada, Y., Kobayashi, K., Miyake, M., Hazama, A., Wada, I., Kanemaru, S., Nakamura, T., and Omori, K. Tissue engineering for regeneration of the tracheal epithelium. Ann Otol Rhinol Laryngol **115,** 501, 2006.
43. Kutten, J.C., McGovern, D., Hobson, C.M., Luffy, S.A., Nieponice, A., Tobita, K., Francis, R.J., Reynolds, S.D., Isenberg, J., and Gilbert, T. Decellularized tracheal extracellular matrix supports epithelial migration, differentiation and function. Tissue Eng Part A **21,** 75, 2015.
44. Neuringer, I.P., Mannon, R.B., Coffman, T.M., Parsons, M., Burns, K., Yankaskas, J.R., and Aris, R.M. Immune cells in a mouse airway model of obliterative bronchiolitis. Am J Respir Cell Mol Biol **19,** 379, 1998.
45. Suh, S.W., Kim, J., Baek, C.H., Han, J., and Kim, H. Replacement of a tracheal defect with autogenous mucosa lined tracheal prosthesis made from polypropylene mesh. ASAIO J **47,** 496, 2001.

Address correspondence to:
Laura E. Niklason, MD, PhD
Department of Biomedical Engineering
Yale University
Room 301D
10 Amistad Street
New Haven, CT 06519

E-mail: laura.niklason@yale.edu

Received: April 5, 2016
Accepted: August 2, 2016
Online Publication Date: September 2, 2016